Phase Drift Compensation of Sub-THz Horn Antenna Pattern in Presence of Phase Center Offset and Orientation Misalignment

Kyung-Won Kim
Terrestrial & Non-Terrestr. Integrat. Telecom. Research Lab.
Electronics and Telecommunications Research Institute
Daejeon, Korea
kimkw@etri.re.kr

Jung-Nam Lee
Terrestrial & Non-Terrestr. Integrat. Telecom. Research Lab.
Electronics and Telecommunications Research Institute
Daejeon, Korea
jnlee77@etri.re.kr

Myung-Don Kim
Terrestrial & Non-Terrestr. Integrat. Telecom. Research Lab.
Electronics and Telecommunications Research Institute
Daejeon, Korea
mdkim@etri.re.kr

***Abstract*—When the phase center of an antenna and the rotation center are not perfectly aligned, phase drift occurs in the antenna pattern measurement. This issue becomes more severe at higher frequencies. This paper presents a method for estimating and compensating for phase center offset, even when the phase center offset is unknown. Additionally, experimental results of horn antenna patterns measured at 159 GHz using the proposed method are provided.**

***Index Terms*—anechoic chamber calibration, antenna pattern measurement, horn antenna, phase center offset, Sub-terahertz (Sub-THz), Terahertz (THz)**

I. Introduction

The millimeter wave frequency bands were allocated for the fifth generation mobile communications (5G) due to their ability to support large bandwidth and dense networks [1]. One of the key technologies that has merged in the 5G landscape is beamforming. Understanding the characteristics of multipath channels is crucial for the harnessing the benefits of beamforming. In millimeter wave channel studies, a major measurement method to overcome the high path loss and measuring multipath channel characteristics involves using a rotating high-gain horn antenna [2], [3]. Additionally, sub-THz frequencies above 100 GHz are being considered as potential frequencies for the sixth generation mobile communications [4]. Previous studies have reported sub-THz channel measurement data using rotating horn antennas [5]. The accuracy of estimating multipath components by synthesizing measurement data in multiple direction directly depends on the precision of antenna pattern measurements [6]. At high frequencies, phase drift easily occurs in a rotating antenna when the rotation center and phase center of the measurement antenna are not aligned. The problem becomes more pronounced above 100 GHz compared to millimeter waves due to the inverse relationship between phase drift and wavelength [7]. This paper presents a method for estimating phase center offset parameters and compensating for phase errors caused by phase center offset and orientation misalignment. The remaining sections of the paper are organized as follows. Section II explains the relationship between phase center offset and phase error. Section III introduces the method for estimating phase center offset and compensatig for phase errors. Section IV provides the results of antenna pattern measurements corresponding compensation. Finally, Section V concludes the paper.

This work was supported by the Institute for Information & communications Technology Promotion (IITP) grant funded by the Korean government (MSIT). (No. 2021-0-00103, "Research and development of technologies for utilization of THz frequency band and evaluation of electromagnetic safety")

II. Phase Drift by Phase Center Offset

A phase error can be estimated based on a propagation length with an antenna center offset. A propagation length can be calculated by

$$\begin{aligned} &d'\left(d, r_{\mathrm{c}}, \theta_{\mathrm{c}}, \phi+\theta_{\mathrm{mis}}\right) \\ &=\sqrt{\left(d-r_{\mathrm{c}} \cos\left(\phi+\theta_{\mathrm{c}}\right)\right)^2+r_{\mathrm{c}} \sin^2\left(\phi+\theta_{\mathrm{c}}\right)}, \end{aligned} \tag{1}$$

where a propagation length, an antenna center offset distance, an antenna center offset direction, and an antenna misalignment angle were denoted by $d'(\cdot)$, r_{c}, θ_{c}, and θ_{mis}, respectively. A recorded boresight direction of a measurement antenna was denoted by ϕ. A distance between a standard horn antenna and the rotation center of a measurement antenna was denoted by d. The antenna position offset parameters are shown geometrically in Fig. 1. A phase error by the antenna phase center offset is expressed by

$$p_{\mathrm{e}}\left(r_{\mathrm{c}}, \theta_{\mathrm{c}}, \phi\right)=\frac{2 \pi d'\left(d, r_{\mathrm{c}}, \theta_{\mathrm{c}}, \phi\right)}{\lambda}, \tag{2}$$

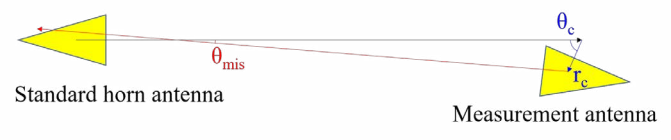

Fig. 1. Parameterization of antenna position offsets

where $p_{\mathrm{e}}(\cdot)$ and λ denoted a phase error and a wave length, respectively.

III. Phase Drift Compensation Algorithm

The antenna position offset parameters were calculated by

$$\left\{r_{\mathrm{c}}^{\mathrm{est}}, \theta_{\mathrm{c}}^{\mathrm{est}}\right\} = \underset{\{r_{\mathrm{c}}, \theta_{\mathrm{c}}\}}{\arg\min}\, J_1\left(r_{\mathrm{c}}, \theta_{\mathrm{c}}, \theta_{\mathrm{mis}}^{\mathrm{est}}\right) \tag{3}$$

and

$$\theta_{\mathrm{mis}}^{\mathrm{est}} = \underset{\theta_{\mathrm{mis}}}{\arg\min}\, J_2\left(\theta_{\mathrm{mis}}\right), \tag{4}$$

where

$$J_1\left(r_{\mathrm{c}}, \theta_{\mathrm{c}}, \theta_{\mathrm{mis}}\right) = \int_{-\pi}^{\pi} \left|\alpha'\left(\phi\right) \cdot \arg\left(\frac{\alpha'\left(\phi\right) \cdot e^{-jp_{\mathrm{e}}\left(r_{\mathrm{c}}, \theta_{\mathrm{c}}, \phi\right)}}{\alpha'\left(\theta_{\mathrm{mis}}\right) \cdot e^{-jp_{\mathrm{e}}\left(r_{\mathrm{c}}, \theta_{\mathrm{c}}, \theta_{\mathrm{mis}}\right)}}\right)\right|^2 d\phi \tag{5}$$

and

$$J_2\left(\theta_{\mathrm{mis}}\right) = \int_{-\pi}^{\pi} \left(\left|\alpha'(\phi - \theta_{\mathrm{mis}})\right| - \left|\alpha'(\theta_{\mathrm{mis}} - \phi)\right|\right)^2 d\phi. \tag{6}$$

The estimated phase center offset distance and direction were denoted by $r_{\mathrm{c}}^{\mathrm{est}}$ and $\theta_{\mathrm{c}}^{\mathrm{est}}$, respectively. The estimated misalignment angle was denoted by $\theta_{\mathrm{mis}}^{\mathrm{est}}$. The antenna pattern measurement was denoted by $\alpha'(\cdot)$ and the proposed cost functions to determine phase center offset parameters were denoted by $J_1(\cdot)$ and $J_2(\cdot)$. The first cost function calculates a weighted sum of squares of relative phase gain. In this calculation, the power gain of each antenna direction is used as the weight for the cost function. This approach minimizes the phase variation in the main lobe, where the power gain is high. The reference direction for the relative phase gains is set as the 0-degree direction, which is the direction where the misalignment is corrected. The misalignment angle is determined using the second cost function, $J_2\cdot$. The second cost function identifies the direction where the antenna pattern becomes the most symmetric function. Using the antenna position offset parameters, the compensated antenna pattern is computed by

$$\alpha\left(\phi - \theta_{\mathrm{mis}}^{\mathrm{est}}\right) = \alpha'\left(\phi\right) \cdot e^{-jp_{\mathrm{e}}\left(r_{\mathrm{c}}^{\mathrm{est}}, \theta_{\mathrm{c}}^{\mathrm{est}}, \phi\right)}, \tag{7}$$

where $\alpha(\cdot)$ denotes the resulting compensated antenna pattern.

IV. Measurement Results

The antenna patterns were measured using a vector network analyzer in an anechoic chamber. The measurements were conducted in the frequency range of 156 GHz to 162 GHz, with intervals of 0.1 GHz. Mi-Wave's standard horn antenna 261D-25/387 was used as the source antenna and for the thru-calibration process. The measurement antennas used were SAR-2309-06-S2, SAR-1532-06-S2, and SAR-1050-06-S2 provided by SAGE Millimeter, Inc. The antennas were positioned at a height of approximately 1 meter, and the distance between them was 1.515 meters. The anechoic chamber was equipped with absorbers to avoid reflections from the antenna rotators, walls, and antenna jigs. During the measurements, the source antenna was fixed while the measurement antenna was rotated at 1-degree intervals within the range of -90 degrees to 90 degrees. Figs 2–7 illustrate the measurement results and the compensation results for the phase center offset at a frequency of 159 GHz. In these figures, the black lines represent the measured antenna pattern, while the red lines represent the compensated results. Following the compensation process, it was observed that the antenna patterns exhibited symmetry, and the phase gain within the main lobe appeared to be flat.

V. Conclusion

At sub-THz frequencies above 100 GHz, even a small phase center offset can result in a significant phase error. To prevent phase drift, it is crucial to align the phase center precisely with the center of rotation. However, achieving exact alignment between the phase center and rotation center can be challenging. In this paper, we propose a method to compensate for phase drift by estimating the offset between the central axis of rotation and the phase center instead of requiring exact alignment. This approach addresses phase drift and simplifies antenna pattern measurement.

References

[1] T. S. Rappaport, S. Sun, R. Mayzus, H. Zhao, Y. Azar, K. Wang, G. N. Wong, J. K. Schulz, M. Samimi, and F. Gutierrez, "Millimeter wave mobile communications for 5G cellular: it will work!," *IEEE Access*, vol. 1, pp. 335–349, 2013.

[2] T. S. Rappaport, G. R. MacCartney, Jr., M. K. Sasami, and S. Sun "Wideband millimeter-wave propagation measurements and channel models for future wireless communication system design,' *IEEE Trans. Communicat.*, vol. 63, no. 9, pp. 3029–3056, 2015.

[3] J. Lee, K.-W. Kim, M.-D. Kim, J.-J. Park, Y. K. Yoon, and Y. J. Chong, "Measurement-based millimeter-wave angular and delay dispersion characteristics of outdoor-to-indoor propagation for 5G millimeter-wave systems,' *IEEE Access*, vol. 7, pp. 150492–150504, 2019.

[4] T. S. Rappaport, Y. Xing, O. Kanhere, S. Ju, A. Madanayake, S. Mandal, A. Alkhateeb, and G. C. Trichopoulos, "Wireless communications and applications above 100 GHz: opportunities and challenges for 5G and beyond," *IEEE Access*, vol. 7, pp. 78729–78757, 2019.

[5] Y. Xing, T. S. Rappaport, "Millimeter wave and Terahertz urban microcell propagation measurements and models," *IEEE Communicat. Letters*, vol. 25, no. 12, pp. 3755–3759, 2019.

[6] X. Wu, C.-X. Wang, J. Sun, J. Huang, R. Feng, Y Yang, and X. Ge, "60-GHz millimeter-wave channel measurements and modeling for indoor office environments," *IEEE Trans. Antenn. Propagat.*, vol. 65, no. 4, pp. 1912–1924, 2017.

[7] J. Svijelj, U. Navsariwala, E. Porrett, and N. Buris, "Correction of antenna phase center offsets in outdoor range measurements," in *IEEE Antenn. Propagat. Society Internat. Symposium. Digest.*, Columbus, OH, 2003.

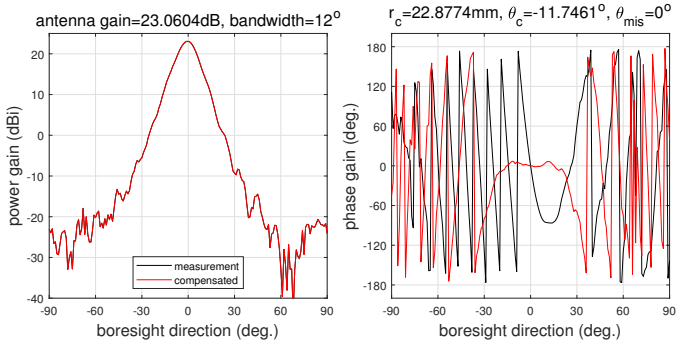

Fig. 2. Position offset compensation results at 159 GHz of 10°-horn Antenna (SAR-2309-06-S2) in the H-plane

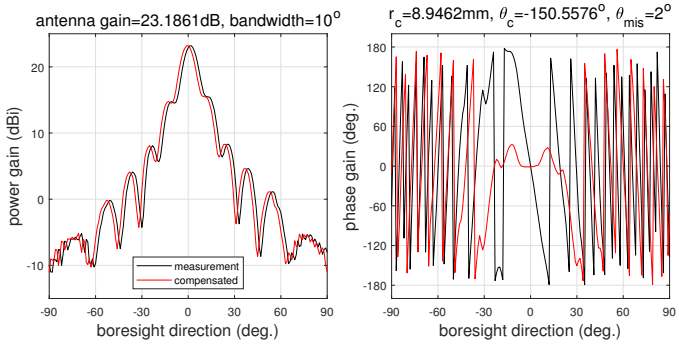

Fig. 3. Position offset compensation results at 159 GHz of 10°-horn Antenna (SAR-2309-06-S2) in the E-plane

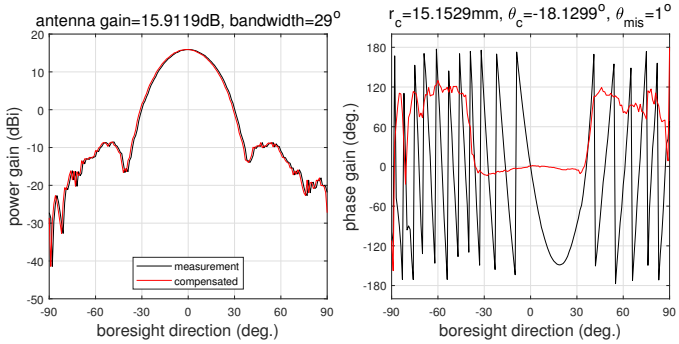

Fig. 4. Position offset compensation results at 159 GHz of 30°-horn Antenna (SAR-1532-06-S2) in the H-plane

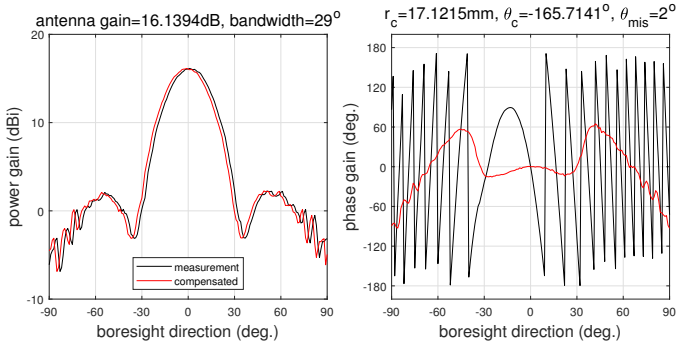

Fig. 5. Position offset compensation results at 159 GHz of 30°-horn Antenna (SAR-1532-06-S2) in the E-plane

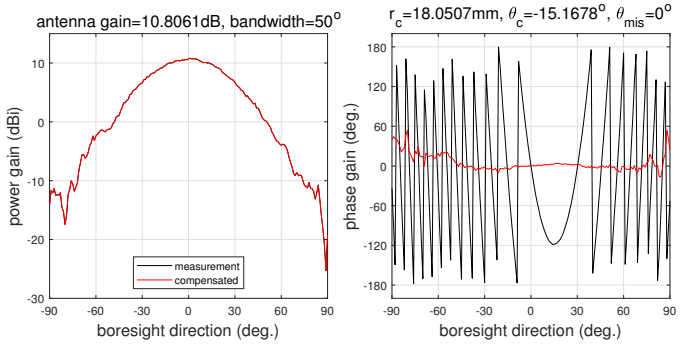

Fig. 6. Position offset compensation results at 159 GHz of 55°-horn Antenna (SAR-1050-06-S2) in the H-plane

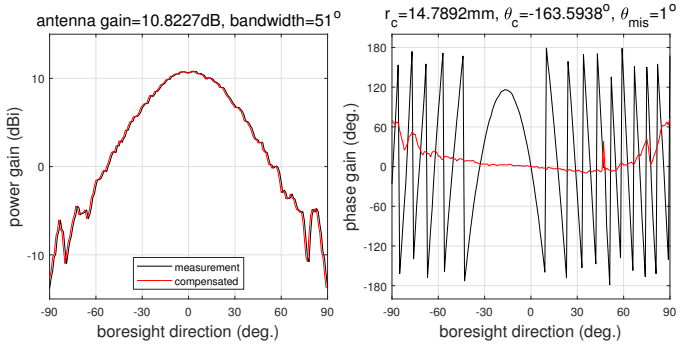

Fig. 7. Position offset compensation results at 159 GHz of 55°-horn Antenna (SAR-1050-06-S2) in the E-plane